第 31 卷第 7 期 无 机 化 学 学 报 Vol.31 No.7
2015 年 7 月 CHINESE JOURNAL OF INORGANIC CHEMISTRY 1278-1286

# 调控从非手性双钯(Ⅱ)和双铂(Ⅱ)配位组装中心同非手性蒽基吡唑配体组装的配位分子角的超分子手性构筑

胡佳华[1] 邓 威[1] 蒋选丰*[,2] 于澍燕*[,1,2]
([1]中国人民大学化学系,自组装化学实验室,北京 100872)
([2]北京工业大学环境与能源工程学院,绿色催化与分离北京市重点实验室,北京 100124)

**摘要**:利用 4-(4-(9-蒽基)苯基)-3,5-二甲基-吡唑配体(L)与不同的双金属组装单元合成了一类新颖的配位分子角[$M_2L_2$]([(bpy)Pd]$_2$$L_2$,**1**;[(dmbpy)Pd]$_2$$L_2$,**2**;[(phen)Pd]$_2$$L_2$,**3**;[(ppy)Pt]$_2$$L_2$,**4**, 其中 bpy=2,2′-联吡啶,dmbpy=4,4′-二甲基-2,2′-联吡啶,phen=1,10-菲咯啉,ppy=2-苯基吡啶)。结果表明这类配位分子角是通过金属-金属成键作用与吡唑基团自发去质子的协同作用自组装形成。利用单晶 X-射线衍射,$^1$H 和 $^{13}$C NMR,ESI-MS 和荧光光谱等测试手段对配合物 **1~3** 的结构进行了测定。同时,电中性的有机金属分子角[(ppy)Pt]$_2$$L_2$ (**4**)的结构也通过 $^1$H 和 $^{13}$C NMR,质谱和荧光光谱等手段进行了表征。运用不同的非手性双金属组装中心同非手性配体 L,自组装得到的 3 个非手性配位分子角的晶体结构差别很大,特别是由[(phen)Pd]$_2$ 组装中心形成的配位分子角 **3** 结晶得到了超分子手性构筑。

**关键词**:分子角;钯(Ⅱ);铂(Ⅱ);超分子手性;金属–金属成键
**中图分类号**:O0614.82$^+$3;O0614.82$^+$6 **文献标识码**:A **文章编号**:1001-4861(2015)07-1278-09
**DOI**:10.11862/CJIC.2015.185

# Tuning Supramolecular Chiral Architecture of Molecular Corners from Achiral Dipalladium(Ⅱ) and Diplatinum(Ⅱ) Complexes with Achiral Anthracyl Pyrazole Ligand

HU Jia-Hua[1] DENG Wei[1] JIANG Xuan-Feng*[,2] YU Shu-Yan*[,1,2]
([1]*Laboratory for Self-Assembly Chemistry, Department of Chemistry, Renmin University of China, Beijing* 100872)
([2]*Beijing Key Laboratory for Green Catalysis and Separation, Department of Chemistry and Chemical Industry, College of Environmental and Energy Engineering, Beijing University of Technology, Beijing* 100124)

**Abstract:** A novel kind of coordination molecular corners [$M_2L_2$] ([**1**=(bpy)Pd]$_2$$L_2$, **2**=[(dmbpy)Pd]$_2$$L_2$, **3**=[(phen)Pd]$_2$$L_2$, **4**=[(ppy)Pt]$_2$$L_2$, where bpy=2,2′-bipyridine, dmbpy=4,4′-dimethyl-2,2′-bipyridine, phen=1,10-phenanthroline, ppy=2-phenylpyridine) was synthesized through synergistic metal-metal bonding interaction and spontaneous deprotonation from the pyrazole linkers 4-(4-(anthracen-9-yl)phenyl)-3,5-dimethyl-1*H*-pyrazole (L). Three complexes **1~3** were characterized by single crystal X-ray diffraction, $^1$H and $^{13}$C NMR, ESI-MS and fluorescence spectroscopy. The neutral organometallic corner [(ppy)Pt]$_2$$L_2$ **4** was also determined by $^1$H and $^{13}$C NMR, MALDI-TOF-MS and fluorescence spectroscopy. These achiral molecular corners assemble from different achiral dimetallic centers with the achiral ligand HL in quite different crystal structures, in particular, **3** with a [(phen)Pd]$_2$ assembling center crystallizes into a supramolecular chiral architecture. CCDC: 1041060, **1**; 1032473, **2**; 1041062, **3**.

**Key words:** molecular corners; palladium (Ⅱ); platinum(Ⅱ); supramolecular chirality; metal-metal bonding interaction

收稿日期:2015-03-31。收修改稿日期:2015-05-31。
国家自然科学基金(No.91127039,21471011)资助项目。
*通讯联系人。E-mail:yusy@ruc.edu.cn

Supramolecular chemistry has attracted a significant research interest due to its rapid expansion to recognization and mimic of biological processes[1-7], molecular devices and machines, host-guest interactions, chemical sensors, dynamic covalent chemistry, catalysis[8], functional materials and medicinal chemistries[9]. Coordination-driven self-assembly, as one of the highly efficient approach for the construction of molecular systems capable of well-defined molecular-level motion, has been a field of growing interest, and a key issue in this field as regards the metal-based molecular corners, tweezers and clefts[10-11], which display fascinating properties and applications, such as catalysis, redox and photoluminescence, etc [12-15]. Therefore, considerable efforts have been devoted to the design and synthesis of functional molecular corners with two 'arms' or 'tips' for host-guest recognition[16-20], molecule separation and purification using various supramolecular interactions including hydrogen bonding, metal coordination, metal-metal bonding, hydrophobic forces, van der waals forces, electrostatic effects and/or $\pi$-$\pi$ interactions[21-24].

Since 2001, we have developed a series of metallic corners complexes[25-27] by combining Pd(Ⅱ) and Pt(Ⅱ) centers with multi-pyrazole anion linkers[28] via metal-metal bonding interactions[29] directed synthesis and spontaneous deprotonation in aqueous solution[30]. These results inspire us to further design new ligands to obtain structurally and functionally novel metal-organic corners[31-33] with promising applications.

By employing a series of bis-Pd(Ⅱ) coordination motifs and anthracyl pyrazolate functional ligands, a new class of "metallic corners" with two rigid pyrazolate pincers in a syn conformation (as shown in Schemes 1 and 2) has been synthesized. NMR, ESI-MS and Elemental analysis technology were used to

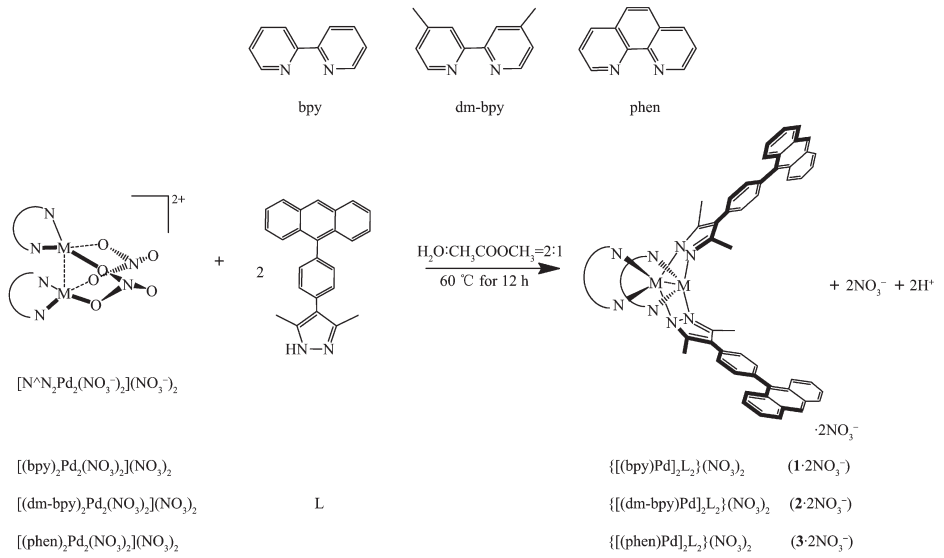


Scheme 1　Synthesis of organometallic "molecular corners" with Pd(Ⅱ)

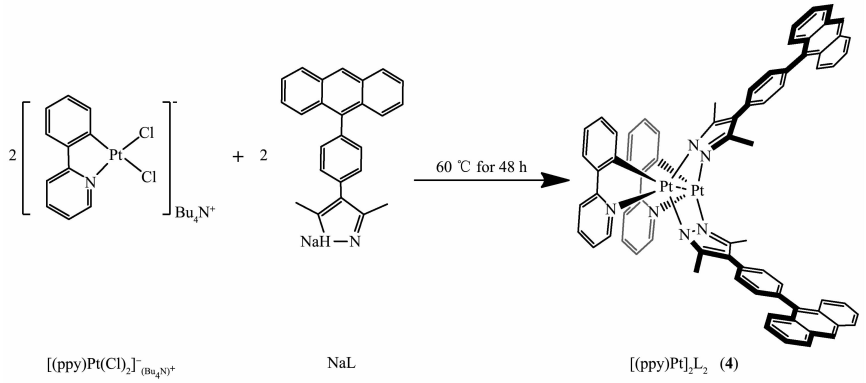


Scheme 2　Synthesis of organometallic "neutral molecular corners" with Pt(Ⅱ)

characterize the structures of the ligand and $[M_2L_2]$ "metallic corners". Complexes $\mathbf{1}\cdot 2PF_6^-$($\mathbf{1}$=$[(bpy)Pd]_2L_2$), $\mathbf{2}\cdot 2PF_6^-$($\mathbf{2}$=$[(dmbpy)Pd]_2L_2$) and $\mathbf{3}\cdot 2PF_6^-$($\mathbf{3}$=$[(phen)Pd]_2L_2$) have also been determined by single-crystal X-ray diffraction structural analysis. Interestingly, the crystallography reveals that the achiral complex $\mathbf{3}\cdot 2PF_6^-$ is self-assembled to a chiral three dimensional packing structure via intermolecular $\pi$-$\pi$ stacking and C–H$\cdots\pi$ hydrogen bonds in the solid state.

## 1 Experimental

### 1.1 Materials and instruments

All chemicals and solvents were of reagent grade and were purified according to conventional methods[34]. The dimetal corners $[(bpy)_2Pd_2(NO_3)_2](NO_3)_2$, $[(dmbpy)_2Pd_2(NO_3)_2](NO_3)_2$, $[(phen)_2Pd_2(NO_3)_2](NO_3)_2$ and $[(ppy)_2Pt_2]Cl_2$ were prepared according to literature procedures[35].

X-ray diffraction measurements were carried out at 291 K on a Bruker Smart Apex CCD area detector equipped with a graphite monochromated Mo $K\alpha$ radiation ($\lambda$=0.071 073 nm). The absorption correction for all complexes was performed using SADABS. All the structures were solved by direct methods and refined by employing full-matrix least-squares on $F^2$ using the SHELXTL (Bruker, 2000) program and expanded using Fourier techniques[36-37]. All non-H atoms of the complexes were refined with anisotropic thermal parameters. The hydrogen atoms were included in idealized positions.

Two visual molecular models were computed using CAChe program 6.1.1[38] to evaluate the shape of metallo-corners **4**.

### 1.2 Synthesis and characterization of $\mathbf{1}\cdot 2PF_6^-$, $\mathbf{2}\cdot 2PF_6^-$, $\mathbf{3}\cdot 2PF_6^-$ and 4

1.2.1 General pyrazole ligand preparation

The pyrazole ligand, 4-(4-(anthracen-9-yl)phenyl)-3,5-dimethyl-1*H*-pyrazole (L), was synthesized using a method similar to that employed for the other known ligands(refer to supporting information for the synthesis). $^1$H NMR (400 MHz, DMSO-$d_6$, 25 ℃, TMS): $\delta$=12.41 (s, 1H, Pz-H), 8.69 (s, 1H, anthryl-H), 8.16 (d, *J*=6.9 Hz, 4H, anthryl-H), 7.66 (d, *J*=6.9 Hz, 4H, anthryl-H), 7.55 (t, *J*=5.6 Hz, 4H, anthryl-H), 7.46 (s, 4H, Ar-H), 2.51 (s, 3H, $CH_3$-H), 2.50 (s, 3H, $CH_3$-H).

1.2.2 Synthesis of complex $\{[(bpy)Pd]_2L_2\}(PF_6)_2$ ($\mathbf{1}\cdot 2PF_6^-$)

$[(bpy)_2Pd_2(NO_3)_2](NO_3)_2$ (9.5 mg, 0.024 mmol) was added to a suspension of L (10 mg, 0.029 mmol) in $H_2O$ and acetone (2 mL, 1:1, *V*/*V*), and the mixture was stirred for 24 h at 85 ℃. The $PF_6^-$ salt of $\mathbf{1}\cdot 2NO_3^-$ was obtained by adding a 10-fold excess of $KPF_6$ to aqueous solution of $\mathbf{1}\cdot 2NO_3^-$ at 60 ℃, which resulted in the immediate deposition of $\mathbf{1}\cdot 2PF_6^-$ as yellow crystals in quantitative yield. The crystals were filtered, washed with a minimum amount of cold water, and dried under vacuum. Yield: 19.0 mg (97%). $^1$H NMR (400 MHz, $CD_3CN$, 25 ℃, TMS): $\delta$=8.65(s, 4H, bpy-H), 8.38 (m, 4H, bpy-H), 8.29 (s, 2H, anthryl-H), 8.17 (d, *J*=8.4 Hz, 8H, anthryl-H), 7.72 (m, 4H, bpy-H), 7.57 (m, 8H, Ar-H), 7.53 (m, 8H, anthryl-H), 7.45 (t, *J*=4.5 Hz, 4H, bpy-H), 2.17 (s, 12H, $CH_3$-H); $^{13}$C NMR (100 MHz, $CD_3CN$, 25 ℃, TMS): $\delta$ 156.76, 150.49, 147.66, 142.26, 136.74, 131.63, 130.00, 120.04, 117.34, 13.02; ESI-MS (acetonitrile, *m*/*z*): 610.1 $[\mathbf{1}]^{2+}$; 1 365.2 $[\mathbf{1}\cdot PF_6]^+$; Elemental analyses Calcd. (%) for $C_{70}H_{54}N_8P_2F_{12}Pd_2\cdot 2H_2O$: C, 54.38; H, 3.78; N, 7.25; Found: C, 53.88; H, 3.75; N,7.12.

1.2.3 Synthesis of complex $\{[(dmbpy)Pd]_2L_2\}(PF_6)_2$ ($\mathbf{2}\cdot 2PF_6^-$)

$(dmbpy)Pd(NO_3)_2$ (11.5 mg, 0.024 mmol) was added to a suspension of L (10 mg, 0.029 mmol) in $H_2O$ and acetone (2 mL, 1:1, *V*/*V*), and the mixture was stirred for 24 h at 85 ℃. The $PF_6^-$ salt of $\mathbf{2}\cdot 2NO_3^-$ was obtained by adding a 10-fold excess of $KPF_6$ to aqueous solution of $\mathbf{2}\cdot 2NO_3^-$ at 60 ℃, which resulted in the immediate deposition of $\mathbf{2}\cdot 2PF_6^-$ as yellow crystals in quantitative yield. The crystals were filtered, washed with a minimum amount of cold water, and dried under vacuum. Yield: 18.7 mg (93%). $^1$H NMR (400 MHz, $CD_3CN$, 25 ℃, TMS): $\delta$=8.61 (s, 4H, dmbpy-H), 8.22 (s, 4H, dmbpy-H), 8.12 (m, 2H, anthryl-H), 7.73 (d, *J*=12.8Hz, 8H, anthryl-H), 7.67 (d, *J*=8.2 Hz, 8H, Ar-H), 7.53(d, *J*=8.8 Hz, 8H, anthryl-H), 7.44 (t, *J*=4.5, 4H, dmbpy-H), 2.17 (s, 24H, $CH_3$-H); $^{13}$C NMR (100 MHz, $CD_3CN$, 25 ℃, TMS): $\delta$ 156.29, 150.00, 147.44,

131.43, 130.08, 128.99, 126.69, 125.70, 124.62, 117.32, 20.76, 13.01; ESI-MS (acetonitrile) *m/z*: 638.15 $[\mathbf{2}]^{2+}$; 1 421.25 $[\mathbf{2}\cdot PF_6]^+$; Elemental analyses Calcd.(%) for $C_{74}H_{62}N_8P_2F_{12}Pd_2\cdot 2H_2O$: C, 55.48; H, 4.15; N, 6.99; Found: C, 55.47; H, 4.18; N, 6.98.

1.2.4　Synthesis of complex $\{[(Phen)Pd]_2L_2\}(PF_6)_2$ ($\mathbf{3}\cdot 2PF_6^-$)

(phen)$Pd(NO_3)_2$ (11.7 mg, 0.024 mmol) was added to a suspension of L (10 mg, 0.029 mmol) in $H_2O$ and acetone (2 mL, 1∶1, *V*/*V*), and the mixture was stirred for 24 h at 85 ℃. The $PF_6^-$ salt of $\mathbf{3}\cdot 2NO_3^-$ was obtained by adding a 10-fold excess of $KPF_6$ to aqueous solution of $\mathbf{3}\cdot 2NO_3^-$ at 60 ℃, resulting in the immediate deposition of $\mathbf{3}\cdot 2PF_6^-$ as yellow crystals in quantitative yield. The crystals were filtered, washed with a minimum amount of cold water, and dried under vacuum. Yield: 19.8 mg (91%). $^1$H NMR (400 MHz, $CD_3CN$, 25 ℃, TMS): $\delta$=8.88 (d, *J*=8.4 Hz, 4H, phen-H), 8.66 (s, 2H, anthryl-H), 8.64 (d, *J*=5.3 Hz, 4H, phen-H), 8.20 (d, *J*=8.4 Hz, 8H, anthryl-H), 8.04(m, 4H, phen-H), 7.79 (d, *J*=6.9 Hz, 8H, Ar-H), 7.58 (m, 8H, anthryl-H), 7.46 (d, *J*=8.4 Hz, 4H, anthryl-H), 2.80 (s, 12H, $CH_3$-H); $^{13}$C NMR (100 MHz, $CD_3CN$, 25 ℃, TMS): $\delta$ 151.61, 147.91, 147.29, 141.03, 131.39, 130.84, 130.07, 129.10, 128.46, 128.11, 127.01, 126.69, 126.38, 125.72, 125.35; ESI-MS (acetonitrile) *m/z*: 633.13 $[\mathbf{3}]^{2+}$, 1 411.2 $[\mathbf{3}\cdot PF_6]^+$; Elemental analyses Calcd.(%) for $C_{74}H_{54}N_8P_2F_{12}Pd_2\cdot 2H_2O$: C, 55.76; H, 3.67; N, 7.03; Found: C, 55.99; H,3.72 ; N,6.94.

1.2.5　Synthesis of complex $[(ppy)Pt]_2L_2$ (**4**)

2-phenyl pyridine platinum chloride (124.3 mg, 0.18 mmol) was added to a suspension of L (189 mg, 0.54 mmol), $Ag(CF_3SO_3)$ (46.508 mg, 0.18 mmol), NaOMe (29.3 mg, 0.54 mmol), $CH_3CN$ and $CH_3OH$ (20 mL, 1∶1, *V*/*V*), and the mixture was stirred for 24 h at 60 ℃ under $N_2$. The product was collected by filtration, frozen overnight, recrystallization to obtain yellow-green product. Yield : 71 mg (87%). $^1$H NMR (400 MHz, $CD_3CN$, 25 ℃, TMS): $\delta$=8.54 (s, 2H, ppy-H), 8.33 (t, *J*=4.0 Hz, 2H, ppy-H), 8.28 (s, 2H, anthryl-H), 8.08 (d, *J*=7.7 Hz, 2H, ppy-H), 7.80 (t, *J*=4.5 Hz, 8H, anthryl-H), 7.57 (m, 8H, Ar-H), 7.50 (d, *J*=7.8 Hz, 2H, ppy-H), 7.48 (m, 2H, ppy-H), 7.43(d, *J*=8.4Hz, 8H, anthryl-H), 7.40 (t, *J*=4. 5Hz, 2H, ppy-H), 7.28 (s, 2H, ppy-H), 7.03 (d, *J*=6.5 Hz, 2H, ppy-H), 2.47 (s, 12H, $CH_3$-H); $^{13}$C NMR (100 MHz, $CD_3CN$, 25 ℃, TMS): $\delta$ 142.26, 136.74, 132.57, 131.62, 130.08, 129.02, 128.47, 126.71, 126.29, 125.71, 124.06, 117.34, 25.06, 13.02; MALDI-TOF (chloroform) *m/z*: 814.3, 1/2 [**4**+2K$^+$]; 1 103.5, [**4**-L+Na$^+$+K$^+$]; Elemental analyses Calcd.(%) for $C_{72}H_{54}N_6Pt_2$: C, 62.06; H, 3.91; N, 6.03; Found: C, 62.54; H, 4.02; N, 5.98.

### 1.3　X-ray crystallography of complex $\mathbf{1}\cdot 2PF_6^-$, $\mathbf{2}\cdot 2PF_6^-$ and $\mathbf{3}\cdot 2PF_6^-$

Final residuals along with unit cell, space group, data collection, and refinement parameters are presented in Table 1 and Table S1~S3.

CCDC: 1041060, $\mathbf{1}\cdot 2PF_6^-$; 1032473, $\mathbf{2}\cdot 2PF_6^-$; 1041062, $\mathbf{3}\cdot 2PF_6^-$.

**Table 1　Crystal structure determination data for complex $\mathbf{1}\cdot 2PF_6^-$, $\mathbf{2}\cdot 2PF_6^-$ and $\mathbf{3}\cdot 2PF_6^-$**

| Formula | $\mathbf{1}\cdot 2PF_6^-$ ($C_{72}H_{57}F_{12}N_9P_2Pd_2$) | $\mathbf{2}\cdot 2PF_6^-$ ($C_{74}H_{62}F_{12}N_8P_2Pd_2$) | $\mathbf{3}\cdot 2PF_6^-$ ($C_{74}H_{54}F_{12}N_8P_2Pd_2$) |
|---|---|---|---|
| Formula weight | 1 551.01 | 1 566.06 | 1 557.99 |
| Color, habit | Yellow, block | Yellow, Chunk | Yellow, Chunk |
| Crystal system | Monoclinic | Triclinic | Monoclinic |
| Space group | $P2_1/n$ | $P\bar{1}$ | $C2$ |
| *a* / nm | 1.279 6(3) | 1.658 80(8) | 2.276 7(5) |
| *b* / nm | 2.702 1(5) | 2.254 50(12) | 1.179 9(2) |
| *c* / nm | 2.141 3(4) | 2.354 84(12) | 2.906 2(6 |
| $\alpha$ / (°) | 90 | 69.981(2) | 90 |
| $\beta$ / (°) | 95.88(3) | 76.762(2) | 104.21(3) |
| $\gamma$ / (°) | 90 | 85.728(2) | 90 |
| Volume / nm$^3$ | 7.365(3) | 8.054 5(7) | 7.568(3) |

Continued Table 1

| | | | |
|---|---|---|---|
| $Z$ | 4 | 4 | 4 |
| Calculated density / ($Mg \cdot m^{-3}$) | 1.399 | 1.291 | 1.367 |
| Absorption coefficient / $mm^{-1}$ | 0.608 | 0.556 | 0.592 |
| $F(000)$ | 3 128 | 3 168 | 3 136 |
| $\theta$ range for data collection / (°) | 2.06 to 29.17 | 2.39 to 25.54 | 2.14 to 26.00 |
| Limiting indices | $-17 \leqslant h \leqslant 17$, $-35 \leqslant k \leqslant 37$, $-29 \leqslant l \leqslant 20$ | $-20 \leqslant h \leqslant 20$, $-28 \leqslant k \leqslant 28$, $-29 \leqslant l \leqslant 29$ | $-28 \leqslant h \leqslant 28$, $-13 \leqslant k \leqslant 14$, $-35 \leqslant l \leqslant 35$ |
| Reflections collected | 65 400 | 156 851 | 69 064 |
| Independent reflections | 19 724 ($R_{int}$=0.046 9) | 32 934 ($R_{int}$=0.087 1) | 14 364 ($R_{int}$=0.068 6) |
| Absorption correction | Empirical | Empirical | Empirical |
| Refinement method | Full-matrix least-squares on $F^2$ | Full-matrix least-squares on $F^2$ | Full-matrix least-squares on $F^2$ |
| Data / restraints / parameters | 19 895 / 0 / 879 | 32 934 / 0 / 1 780 | 14 364 / 1 / 950 |
| Goodness-of-fit on $F^2$ | 1.171 | 1.092 | 1.047 |
| Final $R$ indices [$I>2\sigma(I)$] | $R_1$=0.073 4, $wR_2$=0.188 4 | $R_1$=0.055 8, $wR_2$=0.148 4 | $R_1$=0.047 1, $wR_2$=0.157 7 |

## 2 Results and discussion

### 2.1 Synthesis of pyrazolate ligands

4-(4-(anthracen-9-yl)phenyl)-3,5-dimethyl-1*H*-pyrazole ligand (L) is a new compound and was synthesized using a method similar to that employed for the other known ligands[39-44].

### 2.2 Characterization of the $[M_2L_2]^{2+}$-type corners

Complex **1**·2$PF_6^-$, **2**·2$PF_6^-$ and **3**·2$PF_6^-$ were fully characterized by elemental analysis, NMR spectroscopies, ESI-MS and X-ray crystal structure determination. The $^1H$ and $^{13}C$ NMR analysis of the product confirmed the formation of a single highly symmetrical species, and integration of the signals indicated a 1∶1 ratio of dimetal motifs $[(bpy)_2Pd_2(NO_3^-)_2](NO_3^-)_2$ to the pyrazolate anion $L^-$ in the corner **1**·2$PF_6^-$ (Fig.1). Remarkably, the signals corresponding to the coordinated bpy ligands present a singlet at 8.65, one set of triplets at 7.45 and two multiplets at 8.38, 7.74 in the downfield region of the spectrum. The signals at 8.29, 8.17, 7.47 are attributed to protons of the anthryl-H and 7.57 is attributed to protons of the Ar-H from pyrazole ligand L. Notably, one singlet at 2.17, ascribed to the methyl protons of the pyrazole ligand L, is evident in the upfield region of the spectrum. The formation of **1** is further supported by ESI-MS in Fig.2 showing the mass to charge ratio (*m*/*z*) peaks 610.1, 1 365.0 for $[\mathbf{1}]^{2+}$, $[\mathbf{1}\cdot PF_6]^+$. The other two similar complexes **2**·2$PF_6^-$ and **3**·2$PF_6^-$ are also obtained and characterized by the same method (Fig. S8~S15).

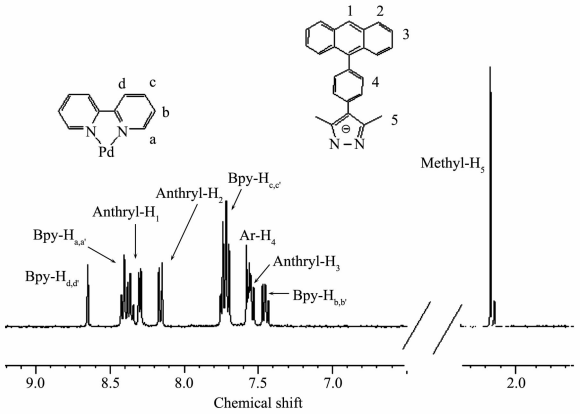


Fig.1 $^1H$ NMR spectrum of **1**·2$PF_6^-$ (400 MHz, $CD_3CN$, 25 ℃, TMS)

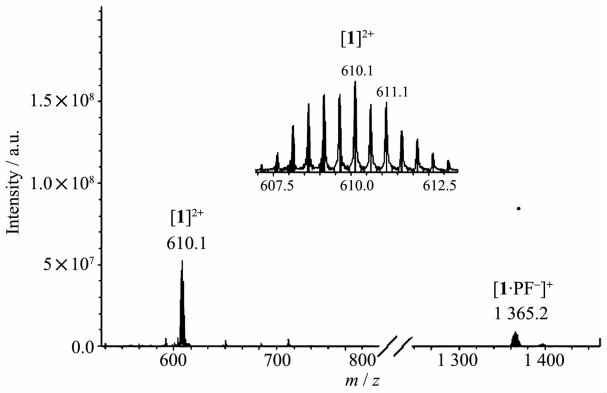


Fig.2 ESI-MS spectrum of **1**·2$PF_6^-$ in acetonitrile; the inset shows the isotopic distribution of the species $[\mathbf{1}]^{2+}$

The $PF_6^-$ salts of all the compounds were obtained by adding 10-fold excess $KPF_6$ to its aqueous solution. By $^1H$ NMR analysis of **1**·$2PF_6^-$, **2**·$PF_6^-$ and **3**·$2PF_6^-$, the positions, integral areas and shaping of the peaks are all understandable. We also have investigated the crystal structures of **1**·$2PF_6^-$, **2**·$2PF_6^-$ and **3**·$2PF_6^-$, which are in consistent to our prospection. As to **4**, the different terminal ligands (ppy) have been adapted to synthesis of neutral metallic molecular corner and we fails to obtain its crystal structure. These structures are fully confirmed by $^1H$ NMR, $^{13}C$ NMR and MALDI-TOF (Fig.S13~S15). All the characterizations have demonstrated that the preparation of these molecular corners as mentioned is successful. The solid state structures of these "metallic corners" have been further confirmed by single crystal X-ray diffraction.

### 2.3 Crystal structure of $[Pd_2L_2]^{2+}$-type corners

The symmetric corner-like structure of complex **1** is strongly supported by single-crystal structure analysis. The structure of **1**·$2PF_6^-$ is shown in Fig.S16 and Fig.S17, complex **1**·$2PF_6^-$ crystallizes in the monoclinic space group $P2_1/n$. The crystallography of **1** reveals the $Pd_2$ dimetallic corner-shaped structure with one ($\mu$-pyrazolato-N,N′)$_2$ doubly-bridged [(bpy)Pd]$_2$ dimetal motifs. In the dimetallic corner, two mono-pyrazole ligands L coordinated with two (bpy)Pd motifs and resulting in the formation of $[Pd_2L_2]$-Type corner. As shown in Fig.S16, two (bpy)Pd moieties are bridged by two pyrazolate ligands in an exodentate fashion. The Pd1…Pd2 separation of 0.315 27(9) nm, which is shorter than that observed in the previous dimetal corner-like complexes, is in the range of typical Pd…Pd interactions (0.26~0.33 nm). The central six membered ring consisting of the two Pd atoms and the four pyrazolyl N atoms has a boat-shaped conformation with Pd-$N_{pz}$ distances between 0.199(6) and 0.202(3) nm and N-Pd-N angles of 77.40° between two pyrazolate groups. Two anthryl groups located at opposed position (dihedral angle is 67.75°) with a distance of 1.392 nm between adjacent central phenyl rings composing of C25-C33 and C13-C18 from two pyrazolate ligands, respectively. The dihedral angle between the two 2,2′-bipyridine terminal ligands (N1-N2 and N3-N4) planes within the corner is 66.36°, which is smaller than the dihedral angle between the pyrazolate ligands. Furthermore, the $Pd_2$ dimetallic corner stacks into a one-dimensional chain via intermolecular $\pi \cdots \pi$ packing interaction and weak C–H$\cdots\pi$ bonds between the aromatic groups of the helices along the crystallographic a axis in the solid state. It is interesting to find that these weak intermolecular interactions between the aromatic rings link dimetal corner together, featuring a three-dimensional network with 1D channels of 1.46 nm×1.48 nm (*i.e.* the distances between the palladium atoms of the adjacent dimetallic corner) containing the $PF_6^-$ anions and solvents.

Complex **2**·$PF_6^-$ crystallizes in the triclinic space group $P\bar{1}$. In the dimetallic corner, two mono-pyrazolate ligands L coordinated with two (dmbpy)Pd motifs and resulting the formation of $[Pd_2L_2]$-type corner. In the asymmetric unit, two molecules of dimetallic assembles as monomer are hold together closely by multiple intermolecular C–H$\cdots\pi$ bonds and formed a "tennis balls" dimer (Fig.S18 and Fig.S19). As shown in Fig.S19, two (dmbpy)Pd motifs are bridged by two pyrazolate ligands in an opening-book fashion and the separation of Pd1…Pd2 is 0.323 2 nm. The pyrazolyl N atoms has a boat-shaped conformation with Pd-$N_{pz}$ distances between 0.199 2 and 0.202 nm and N-Pd-N angles of 85.42° between two pyrazolate groups. Two anthryl groups locate at opposed position (dihedral angle is 83.78°, the center distance is 1.253 nm). The dihedral angle between two adjacent central phenyl rings from two pyrazolate ligands is 69.32° and between the two 4,4′-dimethyl-2,2′-bipyridine terminal ligands (N1-N2 and N3-N4) planes is 77.58°. Furthermore, one $PF_6^-$ anion in the crystal locate in the [(dmbpy)Pd]$_2$ dimetal corner and adjacent to the dmbpy ligands by hydrogen bonds of C–H…F. Interestingly, the dimetal corner could pack into three-dimensional tubular channel with the wall containing the bridged linkers and the dmbpy aromatic rings, which extend in the crystallographic *a*, *b*, and *c* axes with $PF_6^-$ anions frozen inside.

After replacing dimetallic clips $[(bpy)_2Pd_2(NO_3)_2](NO_3)_2$ with $[(phen)_2Pd_2(NO_3)_2](NO_3)_2$, an extremely

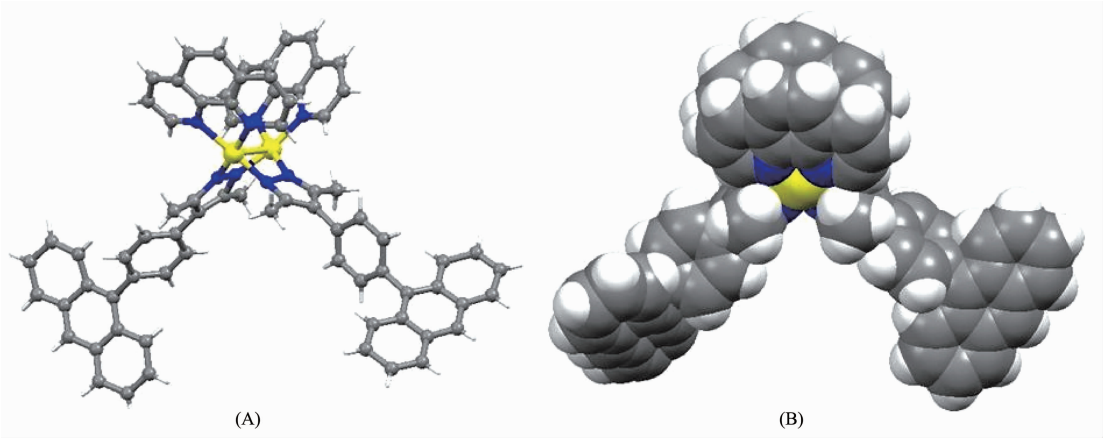


Fig.3 Coordination mode and corners structure of **3**·2$PF_6^-$ drawn in the ball and stick mode from side view; All solvents and counter anions are omitted for clarity

similar assembly is afforded. As shown in Fig.3 and Fig.4, the crystal structure of **3**·2$PF_6^-$ also displays a [$Pd_2L_2$] metal-organic corner structure, and the selected bond lengths and angles are depicted. Complex **3**·2$PF_6^-$ crystallizes in the monoclinic space group *C*2. Like with **1**·2$PF_6^-$ and **2**·2$PF_6^-$, the crystallography of **3**·2$PF_6^-$ reveals the $Pd_2$ dimetallic corner-shaped structure with one ($\mu$-pyrazolato-N,N′)$_2$ doubly-bridged [(phen)Pd]$_2$ dimetal motifs. In the dimetallic corner, two mono-pyrazole ligands L coordinate with two (phen)Pd motifs resulting in [$Pd_2L_2$]-type molecular corner formation. Pd-$N_{pz}$ distances are between 0.188(8) and 0.207(5) nm and N-Pd-N angles of 87.57° between two pyrazolate groups. The Pd1 ⋯ Pd2 separation is 0.306(7) nm. Two anthryl groups locate at opposed position with a dihedral angle of 45.54°. The dihedral angle between two adjacent central phenyl-ring planes from two pyrazolate ligands is 56.70°, and two 1,10-phenanthroline terminal ligands (N1-N2 and N3-N4) planes within the corner is 62.49°. Because of the weak intermolecular $\pi \cdots \pi$ packing interaction and C–H ⋯ $\pi$ bonds between the aromatic groups of the helices along the crystallographic a axis in the solid state, the $Pd_2$ dimetallic corner stacks into a one-dimensional chiral chain (Fig.4). The chirality of the crystals of **3**·2$PF_6^-$ is further confirmed by solid state CD spectroscopy (Fig.S21).

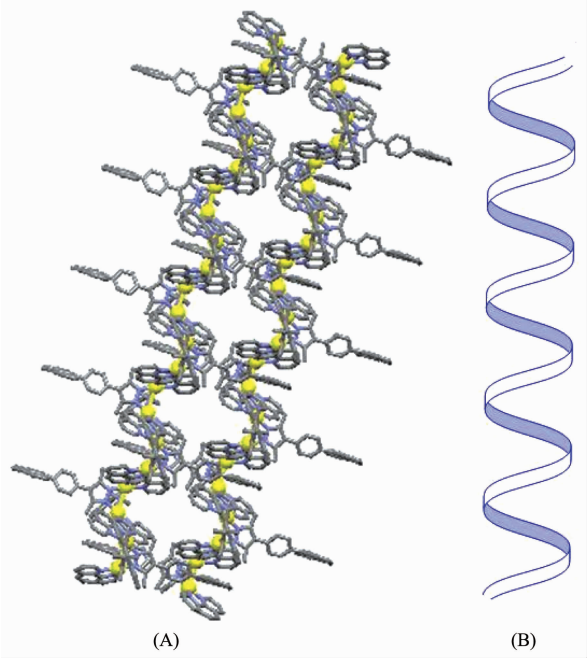


Fig.4 One-dimensional chiral crystallization structure of **3**·2$PF_6^-$ drawn in the spacefilling (A) and simplified packing mode (B)

### 2.4 Spectroscopic properties

The electronic absorption spectra of **1**·2$PF_6^-$, **2**·2$PF_6^-$ and **3**·2$PF_6^-$ (Fig.5) in acetonitrile (**4** in chloroform as shown in Fig.S22) at 298 K exhibit an intense high-energy absorption band at 350~400 nm (blue line,) with an emission shoulder at 400~450 nm (red line). As shown in Fig.5, 12$PF_6^-$ exhibits characteristic anthracene emission and fluorescence maxima at 396, 419 and 437 nm and UV-Vis spectral peaks at 353, 368 and 389 nm in acetonitrile, respectively.

The effects of anions on the fluorescent emission intensity of metallo-corner have been confirmed as shown in Fig.6[45]. The addition of aliquots of $NO_3^-$ to a solution of **3**·2$PF_6^-$ in $H_2O/CH_3CN$ (1:10, *V*/*V*, 1.0×10$^{-5}$

mol·L$^{-1}$) results in a linear increase of the fluorescence intensity until it reaches 1 equiv. concentration ($1.0\times10^{-5}$ mol·L$^{-1}$) (Fig.7). These results preliminary

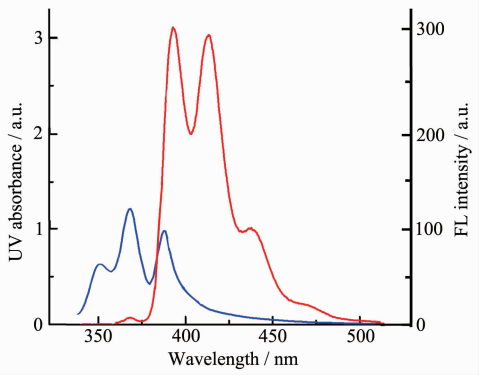


Fig.5 UV-Vis absorption spectrum (the blue line) and the fluorescence emission spectrum (the red line) of **1**·2PF$_6^-$ ($\lambda_{ex}$=368 nm)

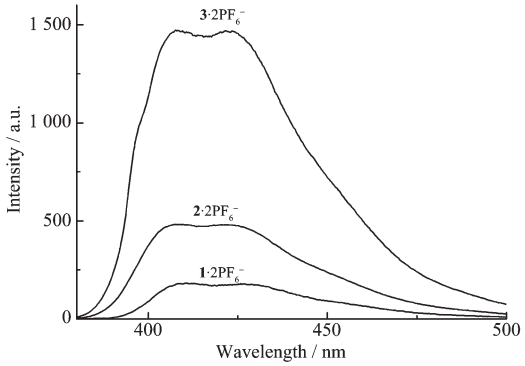


Fig.6 Fluorescence emission spectra of **1**·2PF$_6^-$, **2**·2PF$_6^-$ and **3**·2PF$_6^-$

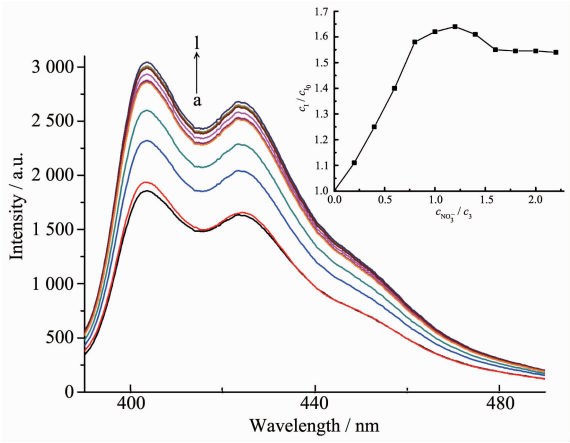


Fig.7 Emission spectral changes of **3**·2PF$_6^-$ ($1\times10^{-5}$ mol·L$^{-1}$) upon addition of different amount of $C_{NO_3^-}$ (black, the fluorescent spectra of 3·2PF$_6$; inset, the plot of the change in $C_{NO_3^-}$, at peak of 403 nm, $\lambda_{ex}$=380 nm); (a) 0, (b) 0.2, (c) 0.4, (d) 0.6, (e) 0.8, (f) 1.0, (g) 1.2, (h) 1.4 ,(i) 1.6, (j) 1.8, (k) 2.0 and (l) 2.2 equiv

reflect the complexing affinity between **3**·2PF$_6^-$ and anions due to the C–H···O hydrogen bonds and electrostatic attraction. However, we failed to obtain the similar change of fluorescence intensity when the addition of $NO^{3-}$ was applied to **1**·2PF$_6^-$ and **2**·2PF$_6^-$, which might be attributed to the weaker C–H···O hydrogen bonds and electrostatic attractions between the anion and host.

## 3 Conclusions

A novel luminescent anthraquinone pyrazole ligand was employed to assemble with Pd(Ⅱ) or Pt(Ⅱ) centers via a directed synthesis process that occurs along with spontaneous deprotonation of the ligands and generates four clip-shaped metallo-corners ($M_2L_2$) in nearly quantitative yield. These fluorescent assemblies have been characterized by elemental analysis, $^1$H and $^{13}$C NMR, ESI-MS and in the cases of **1**·2PF$_6^-$, **2**·2PF$_6^-$ and **3**·2PF$_6^-$ by single crystal X-ray diffraction analysis. Most interestingly, achiral dimetal molecular corner **3**·2PF$_6^-$ self-assembles to a chiral 3D packing structure via weak intermolecular interactions in the solid state.

Supporting information is available at http://www.wjhxxb.cn

**Acknowledgments:** This project was supported by the National Natural Science Foundation of China (No.91127039, 21471011), The Importation and Development of High-Caliber Talents Project of Beijing Municipal Institution, and Beijing Synchrotron Radiation Facility (BSRF) for the crystal structure determination using synchrotron radiation X-ray diffraction analysis.

## References:

[1] Sauvage J P. *Transition Metals in Supramolecular Chemistry, Perspectives in Supramolecular Chemistry*: *Vol.*5. New York: Wiley, **1999**.

[2] Fujita M. *Molecular Self-Assembly Organic Versus Inorganic Approach* (*Structure and Bonding*): *Vol.*96. New York: Springer, **2000**.

[3] Caulder D L, Raymond K N. *Acc. Chem. Res.*, **1999**,**32**:975-982

[4] Navarro J A R, Lippert B. *Coord. Chem. Rev.*, **1999**,**185**-

**186**:653-667

[5] Fujita M, Tominaga M, Hori A, et al. *Acc. Chem. Res.*, **2005**, **38**:371-380

[6] Würthner F, You C C, Saha-Möller C R. *Chem. Soc. Rev.*, **2004**,**33**:133-146

[7] Seidel S R, Stang P J. *Acc. Chem. Res.*, **2002**,**35**:972-983

[8] Kauffman G B. *A Century of Progress, American Chemical Society*: *Vol.*565. Washington DC: Coordination Chemistry, **1994**.

[9] Lehn J M. *Supramolecular Chemistry, Concepts and Perspectives*, Weinheim: VCH, **1995**.

[10]Ballhausen C J. *Introduction to Ligand Field Theory*. New York: McGraw Hill, **1962**.

[11]Atwood J D, Wovkulich M J, Sonnenberger D C. *Acc. Chem. Res.*, **1983**,**16**:350-55

[12]Cotton F A, Walton R A. *Multiple Bonds Between Metal Atoms*, Oxford: Oxford University Press, **1993**.

[13]Cotton F A, Murillo C A, Walton R A. *Multiple Bonds Between Metal Atoms*: 3*rd Ed*. New York: Springer Science and Business Media, Inc., **2005**.

[14]Cotton F A, Lin C, Murillo C A. *Acc. Chem. Res.*, **2001**,**34**: 759-771

[15]Chifotides H, Dunbar K R. *Acc. Chem. Res.*, **2005**,**38**:146-156

[16]Fujita M, Yazaki J , Ogura K. *J. Am. Chem. Soc.*, **1990**,**112**: 5645-5646

[17]Fujita M, Ogura K. *Coord. Chem. Rev.*, **1996**,**148**:249-264

[18]Fujita M. *Chem. Soc. Rev.*, **1998**,**27**:417-426

[19]Fujita M, Umemoto K, Yoshizawa M, et al. *Chem. Commun.*, **2001**:509-518

[20]Fujita M, Tominaga M, Hori A, et al. *Acc. Chem. Res.*, **2005**, **38**:371-380

[21]Alvarez-Vergara M C, Casado M A, Martin M L, et al. *Organometallics*, **2005**,**24**:5929-5935

[22]Baudron S A, Hosseini M W. *Chem. Commun.*, **2008**:4558-4563

[23]Hiraoka S, Sakata Y, Shionoya M J. *Am. Chem. Soc.*, **2008**, **130**:10058-10063

[24]Schmittel M, Mahata K. *Chem. Commun.*, **2008**:2550-2554

[25]Huang H P, Li S H, Yu S Y, et al. *Inorg. Chem. Commun.*, **2005**,**8**:656-660

[26]Ning G H, Yao L Y, Liu L X, et al. *Inorg. Chem.*, **2010**,**49**: 7783-7792

[27]Qin L, Yao L Y, Yu S Y. *Inorg. Chem.*, **2012**,**51**:2443-2453

[28]Yu S Y, Fujita M, Yamaguchi K. *Dalton Trans.*, **2001**:3145-3146

[29]Boixassa A, Pons J, Solans X, et al. *Inorg. Chem. Commun.*, **2003**,**6**:922-925

[30]Yao L Y, Yu Z S, Qin L, et al. *Dalton Trans.*, **2013**:3447-3454

[31]Yu S Y, Jiao Q, Li S H, et al. *Org. Lett.*, **2007**,**9**:1379-1382

[32]Zhang Z X, Huang H P, Yu S Y, et al. *Inorg. Chem.*, **2004**, **20**:849-857

[33]Yu S Y, Huang H P, Li S H, et al. *Inorg. Chem.*, **2005**,**44**: 9471-9488

[34]Conrad R C, Rund J V. *Inorg. Chem.*, **1972**,**11**:129-134

[35]Yu S Y, Fujita M, Yamaguchi K. *Dalton Trans.*, **2001**:3145-3146

[36]Sheldrick G M. *SHELXS*-97, University of Göttingen, **1990**.

[37]Sheldrick G M. *SHELXL*-97 , University of Göttingen, **1997**.

[38]*CA Che* 6.1.1 *for Windows*, Fujitsu Ltd., Chiba, Japan, **2003**.

[39]Tong J, Yu S Y, Li H. *Chem. Commun.*, **2012**,**48**:343-5345

[40]Li S H, Huang H P, Yu S Y, et al. *Chinese J. Chem.*, **2006**, **24**:1225-1229

[41]Sun Q F, Wong K M C, Liu L X, et al. *Inorg. Chem.*, **2008**, **47**:2142-2154

[42]Ezuhar T, Endo K, Aoyama Y. *J. Am. Chem. Soc.*, **1999**, **121**:3279-3283

[43]Pons J, Chadghan A, Casabó J, et al. *Inorg. Chem. Commun.*, **2000**,**3**:296-299

[44]Sakai K, Sato T, Tsubomura T, et al. *Cryst. Struct. Commun. Sect. C*, **1996**,**52**:783-786

[45]Li S H, Huang H P, Yu S Y, et al. *Dalton Trans.*, **2005**: 2346-2348